Journal of Biomolecular NMR (2006) 35: 1–16
DOI 10.1007/s10858-006-0028-4

Article

Interference between cross-correlated relaxation and the measurement of scalar and dipolar couplings by Quantitative J

Eva de Alba* & Nico Tjandra
Laboratory of Molecular Biophysics, National Heart, Lung, and Blood Institute, National Institutes of Health, 50 South Drive, Bethesda, Maryland 20892, USA

Received 13 December 2005; Accepted 27 February 2006

Key words: cross-correlated relaxation, dipolar couplings, dynamic frequency shifts, NMR, scalar couplings

Abstract

The effects of cross-correlated relaxation in Quantitative J methods are analyzed. One-bond ^{1}H–^{13}C scalar and dipolar couplings of protein methine and methylene sites are obtained by monitoring proton and carbon magnetization in Quantitative J experiments. We find that scalar and dipolar couplings of the same pair of nuclei vary depending on the type of magnetization involved. These discrepancies can be as large as several Hz for methylene moieties. The contribution of dynamic frequency shifts, which are known to affect J couplings, is too small to explain the observed differences. We show that processes of magnetization transfer originated by cross-correlated relaxation are largely responsible for these discrepancies. We estimate the error transferred to methylene J values by cross-correlation interference, and show that is close to the experimentally observed one. Furthermore, this analysis indicates that cross-correlated relaxation effects under isotropic and anisotropic media differ, indicating that errors are not cancelled in residual dipolar coupling measurements.

Abbreviations: EDTA – ethylenediaminetetraacetate; HPLC – high pressure liquid chromatography; HSQC – heteronuclear single quantum correlation spectroscopy; INEPT – insensitive nuclei enhancement by polarization transfer

Introduction

Scalar coupling constants provide inter-bond angular information (Bystrov, 1976) and therefore are measured routinely in high-resolution NMR as a means of molecular structure determination. J couplings are also necessary to obtain residual dipolar couplings (RDC), which are powerful tools in biomolecular structure calculation (Prestegard et al., 2000; Bax et al., 2001; de Alba and Tjandra, 2002; Prestegard et al., 2004; Bax and Grishaev, 2005). The importance of J coupling in structural studies deserves to bring into consideration the sources of error in its measurement.

The Quantitative J correlation (Bax et al., 1994) is commonly the method of choice for accurate measurements of J couplings. In the report presented herein we analyze the effect of cross-correlation as a source of error in Quantitative J experiments.

We show that one-bond ^{1}H–^{13}C J values of methine and methylene moieties of the protein ubiquitin vary if proton or carbon magnetization is monitored. These differences are explained by the presence of magnetization transfer and

*To whom correspondence should be addressed.
E-mail: dealbae@nhlbi.nih.gov

dynamic frequency shifts originated by cross-correlated relaxation. We find that the interference between cross-correlation and J coupling is of similar magnitude under isotropic and anisotropic conditions for methine sites, and therefore RDC are only slightly affected by this error in the measurement. In the case of methylene sites the effect of cross-correlated relaxation is substantially different in aligned versus unaligned media and RDC values present larger deviations depending on the type of magnetization involved.

Material and methods

Protein preparation

The preparation of ^{15}N and ^{13}C isotopically enriched ubiquitin and ^{15}N and ^{13}C, ~50% partially deuterated ubiquitin is described in Supplementary Material section (Lazar et al., 1997).

NMR sample preparation and NMR experiments

Lyophilized ubiquitin was dissolved in HPLC grade water (pH adjusted to 3–4), after extensive vortexing and sonication. The solution was then loaded into a PD-10 desalting column (Amersham Biosciences) to eliminate residual salt. NMR samples were prepared at ~2 mM protein concentration determined by weight in ~10% D_2O/H_2O (v/v) solution. The pH was adjusted to 6.6 by adding small amounts of 0.1 M KOH. Protein samples in orienting media were prepared by mixing protein solution with 3:1 DMPC/DHPC (Avanti Polar Lipids) molar ratio to obtain a final bicelle and protein concentration of 5% (w/v) and 4 mM, respectively. The bicelle stock was prepared in 25 mM sodium phosphate buffer at pH 6.6.

NMR experiments were performed at 300 and 308 K on Bruker Avance DRX 800 MHz and DMX 600 MHz spectrometer with triple resonance probe and tri-axial gradients. The pulse sequences used are described in Figure 1. The parameters for NMR experiments are specified in the legend of Figure 1. Signal intensity is modulated with the scalar coupling during $2\delta = 17.84$ ms in the experiment of Figure 1a, and $2T = 28$ ms in the experiment of Figure 1b, by modifying the value of λ, which changes the relative position of the corresponding 180° pulse. Signal intensity was monitored at 20 different values of λ in both experiments.

NMR spectra were processed with NMRPipe (Delaglio et al., 1995) and the peak picking was done with PIPP (Garrett et al., 1991). The software used to obtain normalized intensity values has been reported elsewhere (Ottiger et al., 1998). Once normalized, the intensities were fitted to Equations 2 and 3, for experiments in Figure 1a and b, respectively. Time points were calculated by including the evolution of magnetization during the pulses of finite length for both experiments.

All reported data, excluding the Supplementary Material, were acquired at 800 MHz for ^{15}N, ^{13}C, ~50% ^{2}H-labeled ubiquitin at 308 K, apart from data of Figure 5c, which were acquired at 600 MHz, 308 K for ^{15}N, ^{13}C ubiquitin. Data reported in Supplementary Material include as well experiments performed at 600 MHz, 300 K for non-deuterated ^{15}N, ^{13}C ubiquitin.

Background

For a non-isolated scalar-coupled two-spin system, SI, the in-phase and anti-phase operators resulting from the scalar coupling, S^+ and $2S^+I_z$, relax at different rates. The J value depends on the differential rate of relaxation as shown by Harbison (1993). The dependence of J on the difference of relaxation rates is not related to the illusory effect of splitting reduction caused by line broadening, and it is unrelated to the method or pulse program used (Harbison, 1993).

The larger the difference of the relaxation rates, the smaller the value of the apparent J (Equation 1) (Rexroth et al., 1995).

$$J_{\mathrm{app}} = J - (\Delta R)^2/[(2\pi)^2(2J)] \quad (1)$$

where J_{app} is the apparent scalar coupling constant, J is the coupling constant in the absence of differential relaxation and ΔR is the difference between the transverse relaxation rates of the operators, S^+ and $2S^+I_z$.

If the scalar coupling constant is large in comparison to the difference of the respective operator relaxation rates, this inherent error in J measurement decreases (Rexroth et al., 1995). The operators will interconvert fast during the J evolution period, thus averaging their relaxation rates (Ghose and Prestegard, 1998). This is the case of one-bond

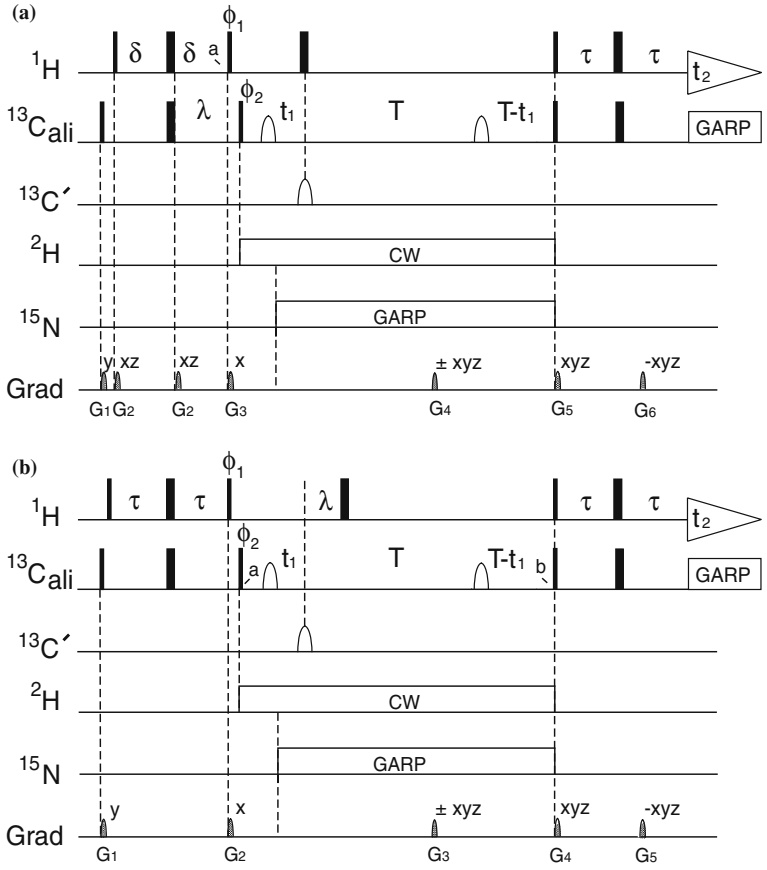

Figure 1. Pulse sequences of the J-modulated [^{1}H–^{13}C]-CT-HSQC experiments monitoring (a) ^{1}H magnetization (Vuister et al., 1993) and (b) ^{13}C magnetization (Ottiger et al., 1998). Narrow and wide rectangles indicate pulses of 90° and 180° flip angles, with phase *x*, unless otherwise indicated. The shaped $^{13}C_{ali}$ pulses, with carrier position at 56 ppm, are of the hyperbolic secant type, with squareness level of 3, and duration of 375.2 μs (Silver et al., 1984). The first $^{13}C_{ali}$ shaped pulse is used to eliminate offset-dependent phase errors caused by the second 180° refocusing pulse. The ^{13}C′ 180° pulse is sine-bell shaped with a duration of $4/\Delta\delta$($\Delta\delta$ is the difference in Hertz between the ^{13}C resonance frequencies of the carrier and the center of the carbonyl region). Delay durations are $\delta = 8.92$ and 14 ms, $\tau = 1.3$ ms, $2T = 28$ and 56 ms. The delay λ is modified 20 times to change the relative position of the 180° pulses in order to modulate signal intensity with the scalar coupling. Phase cycling, $\phi_1 = y, -y$; $\phi_2 = x, x, y, y, -x, -x, -y, -y$ for negative G_4 gradient (Figure 1a) and G_3 gradient (Figure 1b), and $\phi_2 = x, x, -y, -y, -x, -x, y, y$ for the correspondent positive gradients; receiver = $x, -x, y, -y, -x, x, -y, y$. All gradients are sine-bell shaped with 25 G/cm at their center. Gradient durations, for experiment in (a) are $G_{1,2,3,4,5,6} = 4$, 0.2, 3.5, 3.975, 0.7, 0.3 ms, for experiment in (b) are $G_{1,2,3,4,5} = 4$, 3.5, 3.975, 0.7, 0.3 ms. Coherence transfer pathway selection is applied. Quadrature in the t_1 dimension is obtained by acquiring two FIDs with inverted polarity of G_4 (a) and G_3 (b) for each t_1 data. The addition and subtraction of each pair of FIDs provide the two components for quadrature detection (Bachmann et al., 1977). ^{13}C decoupling during ^{1}H acquisition and ^{15}N decoupling during ^{13}C chemical shift evolution is achieved by using GARP (Shaka et al., 1985). In the experiments for ~50% partially deuterated ubiquitin, ^{2}H continuous wave decoupling was used as indicated in the figure.

heteronuclear coupling constants such as ^{1}H–^{13}C (~140 Hz) or ^{1}H–^{15}N in protein amide moieties (~−94 Hz). In contrast, ^{1}H–^{1}H J couplings whose range is ~|1−20| Hz, are affected according to Equation 1. Nevertheless, the mentioned effect can be substantially reduced if ^{1}H–^{1}H J couplings are measured using operators that interconvert fast because they evolve with the sum of a large J and the ^{1}H–^{1}H J, such as zero and double-quantum magnetization (Rexroth et al., 1995).

There are three basic methods commonly used in NMR to obtain scalar coupling constants. One is by measuring the resonance frequency splitting originated by the scalar coupling interaction, for example from E.COSY-type of experiments (Griesinger et al., 1986). Another method relies on the ratio of the peak volume or intensity of signals produced by the in-phase and anti-phase operators that evolve with the scalar coupling (Bax et al., 1994; Tolman and Prestegard, 1996). In the third

method the J values are measured by monitoring the J-modulation of the signal intensity originated by a single operator as a function of time (Vuister et al., 1993; Tjandra and Bax, 1997a; Ottiger et al., 1998). The last two are included in what is commonly known as Quantitative J correlation methods.

Scalar coupling constants measured as frequency splitting are usually affected by inaccuracy in the determination of the frequency values from which the J is derived. Line broadening or partial signal intensity cancellation can produce an artifact shift in the peak maximum.

J couplings determined by the Quantitative J approach that monitors two operators are affected by the difference in the relaxation rates of the magnetizations from which each peak originates (Vuister and Bax, 1993; Grzesiek et al., 1995; Tolman and Prestegard, 1996). Signal intensity or peak volume might be underestimated if relaxation effects are not taken into account, transferring error to the measured J.

In the Quantitative J method that monitors a single operator during a constant time period, the relaxation rate of the operator, in principle, will not change with the modulation. Therefore errors might not be introduced by the presence of different relaxation rates. Additionally, J is not obtained by resonance frequency splitting, thus inaccuracy in the determination of peak frequency is not involved. By considering these issues it seems that the method of Quantitative J from a single operator is less prone to error.

Cross-correlated relaxation between chemical shift anisotropy-dipole (CSA-DD) and dipole–dipole (DD-DD) can affect J measurements differently depending on the method used. When J values are derived from frequency splitting, cross-correlated relaxation modifies the shape of the NMR peaks such that the peak frequency might be inaccurately determined. An apparent instead of the real J value is obtained. This effect has been explained and illustrated in the report by Tjandra and Bax (1997a).

In addition, the imaginary component of the spectral density function associated to CSA-DD cross-correlation induces a change in the scalar coupling, known as dynamic frequency shift (Werbelow, 1996). Dynamic frequency shifts might affect scalar coupling constants measured from resonance splitting and by the Quantitative J approach.

Magnetization can be transferred between operators by CSA-DD and DD–DD cross-correlated relaxation (Werbelow, 1987; Wimperis and Bodenhausen, 1989; Bull, 1991; Ernst and Ernst, 1994; Tjandra et al., 1996; Tessari et al., 1997; Rief et al., 1997; Kroenke et al., 1998; Riek et al., 1999; Carlomagno et al., 1999; Chiarparin et al., 1999; Schwalbe et al., 2001; Boisbouvier and Bax, 2002; Carlomagno et al., 2003). These processes of magnetization transfer can modify the signal intensity in Quantitative J experiments when either one or two operators are monitored. Peak volume or intensity will be under or over-estimated leading to error in the measured J value.

The interference between cross-correlated relaxation and scalar couplings measured by the Quantitative J approach has been commented previously (Tolman and Prestegard, 1996; Tjandra and Bax, 1997a).

It is important though to analyze in detail the effects of cross-correlated relaxation in Quantitative J measurements. This analysis will help to identify possible sources of error, and to estimate its magnitude, which in turn can be experimentally validated. An analysis of these effects might be used to distinguish among errors that are relevant for the measurement of residual dipolar couplings.

Description of pulse programs and analysis of magnetization evolution

One-bond ^{1}H–^{13}C scalar and dipolar couplings of methine and methylene sites were measured with the pulse programs schematically represented in Figure 1. Both experiments are in essence [^{1}H–^{13}C]-CT-HSQC (Santoro and King, 1992) with coherence pathway selection by pulse field gradients (Boyd et al., 1992; Davis et al., 1992; Kay et al., 1992; Tolman et al., 1992). Scalar couplings are obtained from the modulation of ^{1}H transverse magnetization (Figure 1a) and ^{13}C transverse magnetization (Figure 1b) intensity that evolves with J during the period 2λ (Vuister et al., 1993; Ottiger et al., 1998). From now on, experiments of Figure 1a and b will be called H-exp (for proton experiment) and C-exp (for carbon experiment), respectively.

The H-exp is similar to that reported by Vuister et al. (1993) for the measurements of $J(C^{\alpha}-H^{\alpha})$ coupling constants. The modifications mainly include the coherence pathway selection and additional gradients added to suppress artifacts. The C-exp is identical to the one described by Ottiger et al. (1998) for the measurement of scalar and dipolar couplings of protein methine, methylene and methyl moieties.

In the absence of any processes apart from scalar coupling evolution, the signal intensity modulation with time can be described as

$$\text{H-exp: } I = (A_0 \sin(2\pi J\lambda) + A_1)\exp(-A_2(2\lambda)^2) \times \exp(-A_3 2\lambda) \quad (2)$$

$$\text{C-exp: } I = (A_0 \cos(2\pi J\lambda) + A_1)\exp(-A_2(2\lambda)^2) \times \exp(-A_3 2\lambda) \quad (3)$$

where A_0 is the intensity of a reference signal (e.g. 1st time point), A_1 represents the amount of magnetization that does not evolve with J because of imperfections in the π pulses. The Gaussian function, $\exp(-A_2\,(2\lambda)^2)$, takes into account signal intensity decay due to long-range couplings (Ottiger et al., 1998). In both experiments scalar coupling evolution takes place during a constant time module. In spite of this, by including the exponential decay $\exp(-A_3\,2\lambda)$, the fitting of the data to Equation 2 improves with statistical significance as indicated by a p value of 0.02. For Equation 3 the addition of the exponential decay term is irrelevant to the fitting resulting in a p value of 0.94.

When the Quantitative J method from a single operator is used, J values are commonly obtained by fitting the modulation of experimental intensities with time to equations similar to 2 and 3. In the C-exp for methylene groups, the measured scalar coupling will be $J_{CH1} + J_{CH2}$, where H^1 and $H^2$are both geminal protons (Ottiger et al., 1998).

If cross-correlated relaxation takes place while ^1H–^{13}C J coupling is active, magnetization can be transferred between operators, and signal intensity modulation with time might no longer be described by Equations 2 and 3. For the experiments represented in Figure 1a and b we will analyze DD-DD and CSA-DD cross-correlated relaxation for nuclei that are scalar-coupled (or whose scalar coupling evolution is not refocused), and for chemically bonded nuclei, respectively.

By taking into account the effect of π pulses, cross-correlated relaxation takes place during the following times (Schwalbe et al., 2001):

(1) In the H-exp	
1.A. $^{13}C_{CSA}/^1H$–$^{13}C_{DD}$	0
1.B. $^1H_{CSA}/^1H$–$^{13}C_{DD}$	$2(\delta-\lambda)$
1.C. $^1H^i$–$^{13}C^i_{DD}/^1H^i$–$^1H^j_{DD}$	2λ
1.D. $^1H^i$–$^{13}C^i_{DD}/^1H^i$–$^{13}C^j_{DD}$	2δ
(2) In the C-exp	
2.A. $^{13}C_{CSA}/^1H$–$^{13}C_{DD}$	$2(T - t_1-\lambda)$
2.B. $^1H_{CSA}/^1H$–$^{13}C_{DD}$	$2t_1$
2.C. $^{13}C^i$–$^1H^i_{DD}/^{13}C^i$–$^1H^j_{DD}$	$2T$
2.D. $^{13}C^i$–$^1H^i_{DD}/^{13}C^i$–$^{13}C^j_{DD}$	2λ

The superscript "*i*" for the description of three-spin interactions indicates the two nuclei, ^1H and ^{13}C whose one-bond scalar coupling is measured, and "*j*" is the third nucleus coupled to one of them.

All described processes apart from 1.A. might affect the value of J obtained from both C-exp and H-exp.

Magnetization evolution in the H-exp

Starting with magnetization H_y in the product operator formalism (Sörensen et al., 1983), the magnetization that evolves with ^1H–^{13}C coupling at time *a* (Figure 1a) can be described as

$$-H^i_y \cos(2\pi J_{CiHi}\lambda) + 2H^i_x C^i_z \sin(2\pi J_{CiHi}\lambda) \quad (4)$$

The second term of Equation (4) will be collected with the first INEPT step of pulse sequence in Figure 1a. Magnetization that is transferred from any operator to the collected operator during a time that depends on λ, will produce a modulation of the signal intensity that no longer can be accurately described by Equation 2.

Cross-correlated relaxation described by process 1.B can transfer magnetization between operators S^+ and $2S^+I_z$. This type of transfer preserves the phase of the original operator. Therefore, magnetization originated from H^i_y cannot be transferred to the collected operator $2H^i_xC^i_z$. The cross-correlation process described in 1.B, nevertheless, will produce a change in the value of J by the addition of a dynamic frequency shift (Werbelow, 1996):

$$J_{app} = J_r + DFS(^1H_{CSA}/^1H - ^{13}C_{DD}) \quad (5)$$

where J_{app} is the observed value of the coupling, J_r is the real scalar coupling constant and DFS refers to the dynamic frequency shift originated by process 1.B.

In addition to one-bond ^1H–^{13}C coupling, ^1H–^1H coupling is active during the time 2δ in the experiment of Figure 1a. This coupling can be relatively large in the case of methylene moieties.

The evolution of magnetization for example for a CH_2 group can be described as follows:

$$\begin{aligned} &-H_y^i \cos(2\pi J_{CiHi}\lambda)\cos(2\pi J_{HiHj}\delta) \\ &\quad + 2H_x^i H_z^j \cos(2\pi J_{CiHi}\lambda)\sin(2\pi J_{HiHj}\delta) \\ &\quad + 2H_x^i C_z^i \sin(2\pi J_{CiHi}\lambda)\cos(2\pi J_{HiHj}\delta) \\ &\quad + 4H_y^i C_z^i H_z^j \sin(2\pi J_{CiHi}\lambda)\sin(2\pi J_{HiHj}\delta) \end{aligned} \quad (6)$$

Dipole–dipole cross-correlation processes of the type 1.C (e.g. C^β–$H^{\beta 1}_{DD}$/$H^{\beta 1}$–$H^{\beta 2}_{DD}$. Figure 2a) can transfer magnetization between the operators, $2H_x^iC_z^i$ and $2H_x^iH_z^j$. By considering the evolution of magnetization in the presence of this process, the collected operator at point *a* in Figure 1a will be described by

$$\begin{aligned} &2H_x^iC_z^i[\sin(2\pi J_{CiHi}\lambda)\cos(2\pi J_{HiHj}\delta) \\ &\quad \times \cosh(\Gamma_{HiCi/HiHj}2\lambda) - \cos(2\pi J_{CiHi}\lambda) \\ &\quad \times \sin(2\pi J_{HiHj}\delta)\sinh(\Gamma_{HiCi/HiHj}2\lambda)] \end{aligned} \quad (7)$$

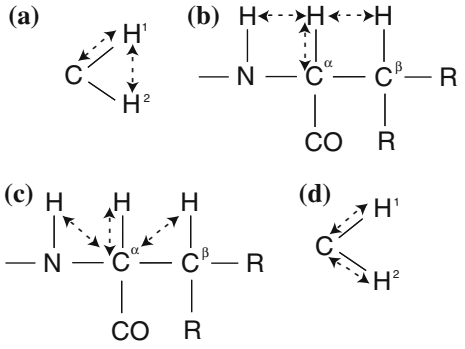

Figure 2. Schematic representation of the DD–DD interactions. Arrows indicate the interacting vectors and the nuclei involved. (a) Dominant pathway of cross-correlated relaxation in the methylene group for the H-exp. (b, c) Two possible interactions in the C^α–H^α moiety of an amino acid containing a single H^β proton in the H-exp and the C-exp, respectively. (d) Dominant DD–DD interaction in methylene moieties in the C-exp.

where $\Gamma_{HiCi/HiHj}$ is the cross-correlated relaxation rate between the $^1H^i$–$^{13}C^i$ and $^1H^i$–$^1H^j$ dipoles (Figure 2a). Because of the large $\Gamma_{HiCi/HiHj}$ in CH_2 moieties this process will be dominant as a source of error in the one-bond J(^1H–^{13}C) for methylene groups (*vide infra*).

For methine groups, a single cross-correlated relaxation pathway might not dominate and several processes need to be taken into account. In order to simplify the equations we can consider as an example the case of C^α–H^α moieties of residues with one beta proton and include two ^1H–^1H couplings not separated by more than three bonds. This means, $^1H^i$ (H^α) coupled to $^{13}C^i$ (C^α), is also coupled to $^1H^j$ (H^β) and $^1H^k$ (H^N). The ^1H–^1H couplings that we consider are $^3J_{H^N–H^\alpha}$ and $^3J_{H^\alpha–H^\beta}$. Dipole–dipole cross-correlated relaxation between $^1H^i$–$^{13}C^i_{DD}$/$^1H^i$–$^1H^j_{DD}$ and $^1H^i$–$^{13}C^i_{DD}$/$^1H^i$–$^1H^k_{DD}$ is effective during the time 2λ. This can be the case of a C^α–H^α dipole, which relaxes by cross-correlation with the H^α–H^N and H^α–H^β dipoles (Figure 2b). Thus the magnetization collected at point *a* in Figure 1a will be described by the following equation:

$$\begin{aligned} &2H_x^iC_z^i[\sin(2\pi J_{CiHi}\lambda)\cos(2\pi J_{HiHj}\delta) \\ &\quad \times \cos(2\pi J_{HiHk}\delta)\cosh(\Gamma_{HiCi/HiHj}2\lambda) \\ &\quad \times \cosh(\Gamma_{HiCi/HiHk}2\lambda) \\ &\quad - \cos(2\pi J_{CiHi}\lambda)\sin(2\pi J_{HiHj}\delta)\cos(2\pi J_{HiHk}\delta) \\ &\quad \times \sinh(\Gamma_{HiCi/HiHj}2\lambda) \\ &\quad - \cos(2\pi J_{CiHi}\lambda)\cos(2\pi J_{HiHj}\delta)\sin(2\pi J_{HiHk}\delta) \\ &\quad \times \sinh(\Gamma_{HiCi/HiHk}2\lambda)] \end{aligned} \quad (8)$$

where $\Gamma_{HiCi/HiHj}$ and $\Gamma_{HiCi/HiHk}$ are the dipole–dipole cross-correlated relaxation rates between $^1H^i$–$^{13}C^i_{DD}$/$^1H^i$–$^1H^j_{DD}$ and $^1H^i$–$^{13}C^i_{DD}$/$^1H^i$–$^1H^k_{DD}$ Figure 2b).

Analogous equations can be derived for the evolution of magnetization in the presence of the cross-correlated relaxation processes described in 1.D.

Magnetization evolution in the C-exp

The magnetization at point *a* (Figure 1b) is represented by the operator $2C_yH_z$. In the case of a methine this operator will evolve with scalar coupling as

$$2C_y^i H_z^i \cos(2\pi J_{\mathrm{CiHi}}\lambda) - C_x^i \sin(2\pi J_{\mathrm{CiHi}}\lambda) \qquad (9)$$

Only the operator at the left-hand side of Equation 9 will be collected. By evolution under ^{13}C chemical shift during t_1 the operators, $-C_y^i \sin(2\pi J_{\mathrm{CiHi}}\lambda)\sin(2\omega_{\mathrm{Ci}}t_1)$ and $2C_y^i H_z^i \cos(2\pi J_{\mathrm{CiHi}}\lambda)\cos(2\omega_{\mathrm{Ci}}t_1)$, are created. Magnetization transferred from the first to the second operator through $^{13}\mathrm{C}_{\mathrm{CSA}}/^{1}\mathrm{H}$–$^{13}\mathrm{C}_{\mathrm{DD}}$ cross-correlated relaxation (process 2.A), will create a dispersive signal in the indirect dimension, since $2C_y^i H_z^i$ will be modulated with $\cos(2\omega_{\mathrm{Ci}}t_1)$, and $\sin(2\omega_{\mathrm{Ci}}t_1)$ from the donor operator. By selecting the maximum of the peak off the real maximum, we have checked experimentally that this is a negligible effect in the value of J.

Analogously to the H-exp, processes 2.A and 2.B will modify the value of J by the presence of dynamic frequency shifts (Werbelow, 1996).

$$J_{\mathrm{app}} = J_{\mathrm{r}} + \mathrm{DFS}(^{1}\mathrm{H}_{\mathrm{CSA}}/^{1}\mathrm{H}-^{13}\mathrm{C}_{\mathrm{DD}}) + \mathrm{DFS}(^{13}\mathrm{C}_{\mathrm{CSA}}/^{1}\mathrm{H}-^{13}\mathrm{C}_{\mathrm{DD}}) \qquad (10)$$

where J_{app} is the observed value of the coupling, J_{r} is the real coupling constant and DFS refers to the dynamic frequency shifts originated by processes 2.A and 2.B.

In addition to the one-bond heteronuclear coupling, ^{13}C is coupled to other protons. For simplicity we will include one additional ^{13}C–^{1}H coupling in the evolution of the magnetization:

$$\begin{aligned} &2C_y^i H_z^i \cos(2\pi J_{\mathrm{CiHi}}\lambda)\cos(2\pi J_{\mathrm{CiHj}}\lambda) - 4C_x^i H_z^i H_z^j \\ &\quad\times \cos(2\pi J_{\mathrm{CiHi}}\lambda)\sin(2\pi J_{\mathrm{CiHj}}\lambda) \\ &\quad- C_x^i \sin(2\pi J_{\mathrm{CiHi}}\lambda)\cos(2\pi J_{\mathrm{CiHj}}\lambda) \\ &\quad- 2C_y^i H_z^j \sin(2\pi J_{\mathrm{CiHi}}\lambda)\sin(2\pi J_{\mathrm{CiHj}}\lambda) \end{aligned} \qquad (11)$$

By the presence of cross-correlated relaxation described in 2.C (e.g. C^{α}–$\mathrm{H}^{\alpha}{}_{\mathrm{DD}}/\mathrm{C}^{\alpha}$–$\mathrm{H}^{\beta}{}_{\mathrm{DD}}$, Figure 2c), magnetization can be transferred between the operators, $2C_y^i H_z^i$ and $2C_y^i H_z^j$. The collected operator at point *b* (Figure 1b) will be described as

$$\begin{aligned} &2C_y^i H_z^i[\cos(2\pi J_{\mathrm{CiHi}}\lambda)\cos(2\pi J_{\mathrm{CiHj}}\lambda) \\ &\times \cosh(\Gamma_{\mathrm{HiCi/CiHj}}2T) \\ &+ \sin(2\pi J_{\mathrm{CiHi}}\lambda)\sin(2\pi J_{\mathrm{CiHj}}\lambda) \\ &\times \sinh(\Gamma_{\mathrm{HiCi/CiHj}}2T)] \end{aligned} \qquad (12)$$

where $\Gamma_{\mathrm{HiCi/CiHj}}$ is the cross-correlated relaxation rate between the $^{1}\mathrm{H}^{i}$–$^{13}\mathrm{C}^{i}$ and $^{13}\mathrm{C}^{i}$–$^{1}\mathrm{H}^{j}$ dipoles (Figure 2c).

For the case of a methylene site two operators are collected at time *a* in Figure 1b, which evolve with scalar coupling as shown in Equation 13:

$$\begin{aligned} &2C_y^i H_z^{i1}\cos[2\pi(J_{\mathrm{CiHi1}} + J_{\mathrm{CiHi2}})\lambda] \\ &\quad + 2C_y^i H_z^{i2}\cos[2\pi(J_{\mathrm{CiHi1}} + J_{\mathrm{CiHi2}})\lambda] \end{aligned} \qquad (13)$$

where H^{i1} and H^{i2} are both methylene protons. Cross-correlated relaxation between C^{i}–H^{i1} and C^{i}–H^{i2} dipoles (Figure 2d) transfers magnetization between the operators represented in Equation 13. The collected magnetization for the first operator at time *b* in Figure 1b can be described as

$$\begin{aligned} &2C_y^i H_z^{i1}\cos[(2\pi(J_{\mathrm{CiHi1}} + J_{\mathrm{CiHi2}})\lambda] \\ &\quad\times [\cosh\Gamma_{\mathrm{CiHi1/CiHi2}}2T - \sinh\Gamma_{\mathrm{CiHi1/CiHi2}}2T] \end{aligned} \qquad (14)$$

where $\Gamma_{\mathrm{CiHi1/CiHi2}}$ is the cross-correlated relaxation rate between the $^{13}\mathrm{C}^{i}$–$^{1}\mathrm{H}^{i1}$ and $^{13}\mathrm{C}^{i}$–$^{1}\mathrm{H}^{i2}$ dipoles of the methylene group (Figure 2d). An analogous expression can be derived for the second operator by changing $2C_y^i H_z^{i1}$ for $2C_y^i H_z^{i2}$.

In addition, ^{13}C is coupled to other directly attached ^{13}C during the constant time period (2T) set to $\sim n\ 1/\mathrm{J_{CC}}$, for $\mathrm{J_{CC}} \sim 35$ Hz ($n = 1, 2, \ldots$). Carbonyl coupling is refocused by the application of a selective π pulse. The description of the magnetization under ^{13}C–^{13}C coupling evolution and cross-correlated relaxation processes of the type 2.D can be derived analogously to process 2.C.

Results

Figure 3a and b show the goodness of the fitting to Equations 2 and 3 of the experimentally observed intensities for the $\mathrm{C}^{\alpha}-\mathrm{H}^{\alpha}$ signal of A_{46} in ubiquitin obtained from the H-exp and C-exp. The fittings of CH and CH_2 groups typically result in values of the reduced χ^2 close to 1, with standard deviation of the intensity of ~0.03 obtained by reproducibility. Notice that a change in the periodicity of the sine and cosine functions is directly related to the obtained J value. Therefore, relaxation processes that affect the periodicity of the sine and cosine functions, and not only their decay, will modify the value of J.

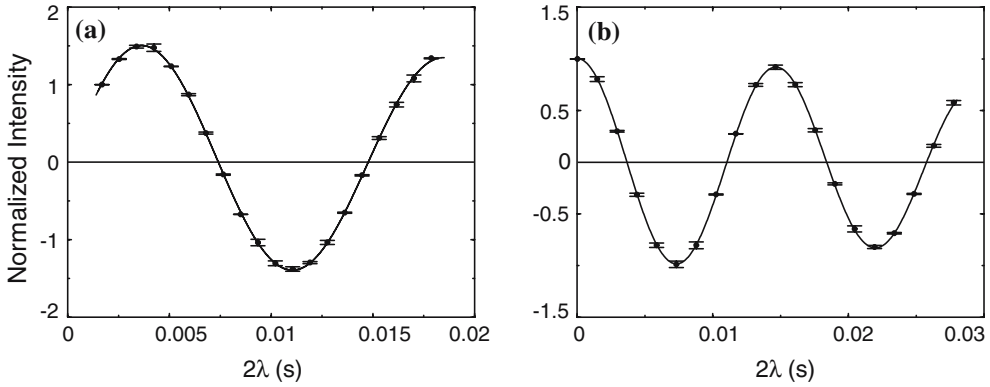

Figure 3. Fitting of the normalized experimental intensity modulated with time for the C^{α}–H^{α} group of ubiquitin A_{46} to (a) Equation 2 for the H-exp, and (b) Equation 3 for the C-exp. Error bars correspond to normalized errors obtained by reproducibility.

The measured one-bond J(C^{α}–H^{α}) couplings using the fitting to Equations 2 and 3 from each experiment are plotted in Figure 4a. J values for methylene sites (including alpha moieties of glycine residues, beta, gamma and delta groups) are shown in Figure 4b. It can be observed that for methine sites the J values obtained from the H-exp are in average 0.8 Hz smaller than from the C-exp, while for methylene groups the J values measured from the H-exp are 4.5 Hz larger than those obtained from the C-exp. The errors by reproducibility in the H-exp measurements are 0.3 and 0.6 Hz for methine and methylene moieties. For the C-exp these errors are 0.3 and 0.4 Hz, respectively. No systematic deviation was observed in either experiment.

Figure 5 shows one-bond J couplings of methine (Figure 5a) and methylene (Figure 5b) sites obtained from the H-exp using two different constant time periods (~18 and 28 ms). At longer constant times, J values of methines decrease, whereas J values of methylene sites increase. In contrast to the H-exp, Figure 5c shows that there is no systematic deviation in the J values measured with the C-exp by increasing the constant time from 28 to 56 ms.

In order to investigate if the differences in the results for methylene groups between the H-exp and the C-exp are related to the presence of two ^{1}H nuclei attached to the same ^{13}C nucleus, we have measured J values using ~50% fractionally deuterated ubiquitin. Three species can be observed in the [^{1}H–^{13}C]-CT-HSQC spectra corresponding to $CH^{1}H^{2}$, $CH^{1}D$ and CDH^{2} groups. Figure 6 represents a portion of the C-experiment showing G_{35} as an example. The different ^{13}C and

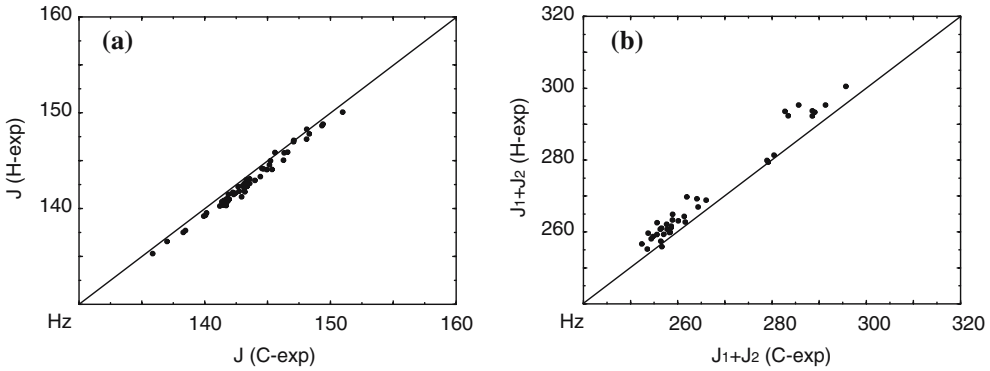

Figure 4. Comparison between the one-bond J(C–H) couplings of ubiquitin (a) C^{α}–H^{α} groups and (b) CH_2 groups, obtained from the H-exp and the C-exp. Note that for methylene moieties only the sum of both couplings is obtained using the C-exp, therefore the J values from the H-exp are added for the comparison.

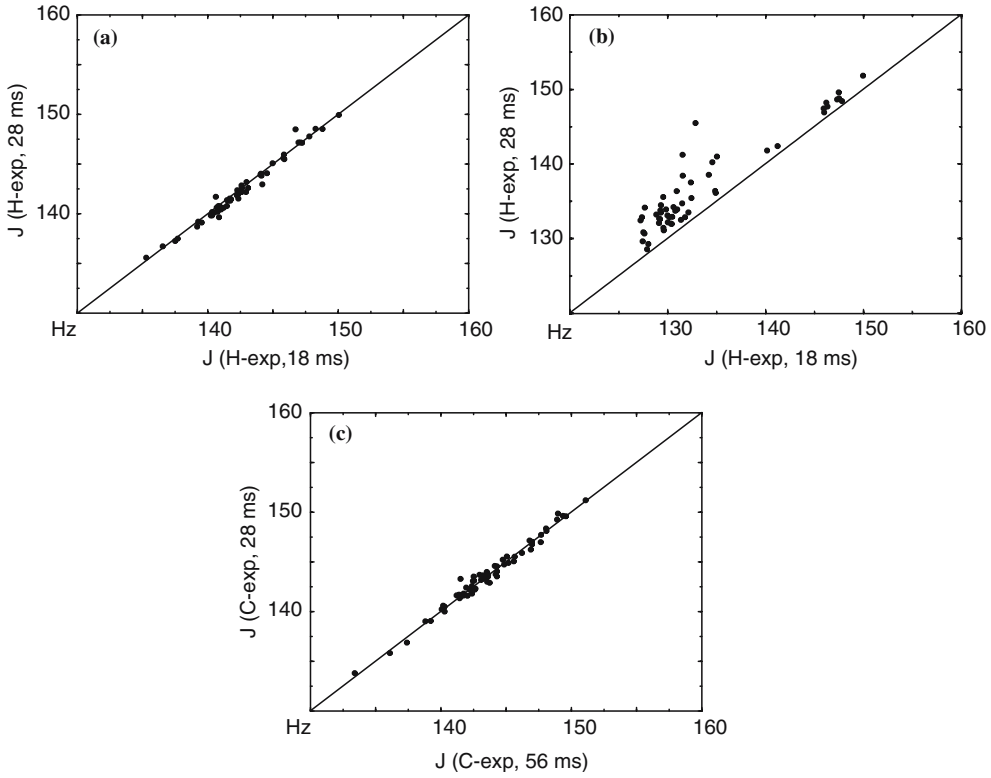

Figure 5. Comparison of the one-bond J(C–H) couplings of ubiquitin (a) C^{α}–H^{α} sites and (b) CH_2 groups, measured with the H-exp at two different values of the constant time 2δ. (c) J of C^{α}–H^{α} moieties from the C-exp at two values of the constant time 2T.

^{1}H chemical shifts in each species are due to the isotope effect originated by the ^{2}H.

Figure 7a and b show the change in J values obtained from the H-exp and C-exp for CHD groups, and CHD vs. CH_2 groups, respectively. It can be observed that the differences between the H-exp and the C-exp for CHD sites are now similar to those found for methine moieties (Figure 4a). J values of CHD and CH_2 groups measured with the C-exp do not change (Figure 7c). In contrast, J data of CHD moieties from the H-exp decrease significantly in comparison to CH_2 sites. These results indicate that the presence of two protons attached to the same ^{13}C is related to larger J values measured with the H-exp.

Figure 8a and b show RDC values obtained from the H-exp and the C-exp for methine and methylene moieties, respectively. RDC were calculated by subtracting J from J + D values obtained under isotropic and anisotropic conditions at the same temperature. It can be observed that the difference in RDC measurements between the H-exp and the C-exp from methine groups is almost cancelled, although there is still some residual deviation. In contrast, large variations are found when comparing RDC data from the H-exp and the C-exp for methylene groups. The observed differences are significantly larger than the experimental errors associated to RDC measurements of CH_2 groups using the H-exp and the C-exp, which are 1.3 and 1.2 Hz, respectively. This result indicates that the measurements under isotropic and anisotropic conditions are affected by different errors, and therefore they do not cancel when obtaining RDC by subtraction.

All J and RDC values are reported for ~50% fractionally ^{2}H-labeled ubiquitin, apart from data shown in Figure 5c (non-deuterated ubiquitin). The same differences were obtained for non-deuterated ubiquitin (data not shown), except for CHD groups, which cannot be measured with this sample. In the Supplementary Material section tables are provided, which include all measured J and RDC values shown in Figures 4–8.

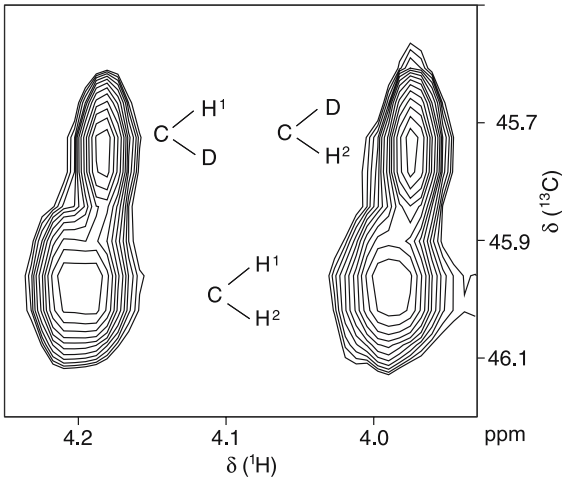

Figure 6. Portion of the [^{1}H–^{13}C]-CT-HSQC showing the three possible species observed for the CH_2 group of G_{35} when using ~50% deuterated ubiquitin.

Discussion

Analysis of the interference between cross-correlated relaxation and J values for methylene moieties

As already demonstrated by the data shown in the previous section, an interaction between the three spins present in methylene groups is responsible for the larger J values measured with the H-exp vs. the C-exp (4.5 Hz at 18 ms). For methylene moieties we will consider first the effect of DD-DD cross-correlated relaxation between the $^1H^i$–$^{13}C^i$ and $^1H^i$–$^1H^j$ dipoles described in 1.C (Figure 2a). This interaction is likely to be dominant due to its large cross-correlated relaxation rate (*vide infra*).

Cross-correlated relaxation rates can be calculated using the following equation:

$$\Gamma_{\mathrm{HiCi/HiHj}} \approx (\tau_c/5)S^2(\mu_0/4\pi)^2(h/2\pi)^2(\gamma_H)^3 \times \gamma_C d_{\mathrm{Ci-Hi}}^{-3} d_{\mathrm{Hi-Hj}}^{-3}(3\cos^2\theta - 1) \quad (15)$$

where τ_c is the overall correlation time of the protein, S^2 is the effective order parameter that takes into account internal motion (Lipari and Szabo, 1982) of the CH_2 group, μ_0 is the susceptibility of the vacuum, γ_H and γ_C, are the gyromagnetic ratios of ^{1}H and ^{13}C, respectively, $d_{\mathrm{Ci\text{-}Hi}}$ and $d_{\mathrm{Hi\text{-}Hj}}$ are the ^{1}H–^{13}C distance and ^{1}H–^{1}H distance in the CH_2 group, θ is the angle between these two vectors (Figure 2a).

The use of Equation 15 to obtain cross-correlated relaxation rates is a simplification since we assume that the overall motion is fully isotropic. In addition, a separation of the internal dynamics of the DD–DD interaction from the geometrical terms relating the relative orientation of this interaction is done by the incorporation of an effective order parameter. For the purpose of this analysis we believe that these simplifications are valid. The value of $\Gamma_{\mathrm{HiCi/HiHj}}$ for CH_2 groups in ubiquitin at 308 K using Equation 15 and an average S^2 value of 0.77 (Jin et al., 2003) is 9.7 Hz. This result can be scaled to ~23 Hz for a protein of ~20 KD. A similar average value of $\Gamma_{\mathrm{HiCi/HiHj}}$ for CH_2 moieties has been reported for a protein of ~20 KD at the same temperature (~27 ± 3 Hz), that was calculated experimentally from the linewidth of CH_2-TROSY experiments (Miclet et al., 2004). In addition, this simplification has been successfully used to extract χ_1 angles and S^2 values of the protein ubiquitin from experimentally determined cross-correlated relaxation rates (Carlomagno et al., 2003).

As commented above, cross-correlated relaxation processes can transfer magnetization to the collected operator. The transfer might modify the periodicity of the intensity modulation with time, changing the value of J. To illustrate this effect we have simulated the intensity from the H-exp using a sine function of the form $\sin(2\pi J\lambda)$ and Equation 7 for a J value of 140 Hz for CH_2 groups. Figure 9 shows the simulated intensity using the regular sine modulation, where cross-correlated relaxation is not considered, and using Equation 7, for which $^1H^i$–$^{13}C^i_{DD}$/$^1H^i$–$^1H^j_{DD}$ is included (Figure 2a). The rest of the parameters used in the simulation are specified in the legend of Figure 9. The periodicity of the curve obtained by taking cross-correlation into account is smaller than that of the curve not including this effect. This means that J values obtained by using Equation 2 ($\propto \sin(2\pi J\lambda)$) to fit intensities that are affected by cross-correlated relaxation will be larger than the real J values.

In Table 1 we report J values obtained by fitting to Equation 2 (that does not consider cross-correlated relaxation) intensities that were simulated using Equation 7 (in which cross-correlated relaxation illustrated in Figure 2a is taken into account). Column 3 shows the J values used in the

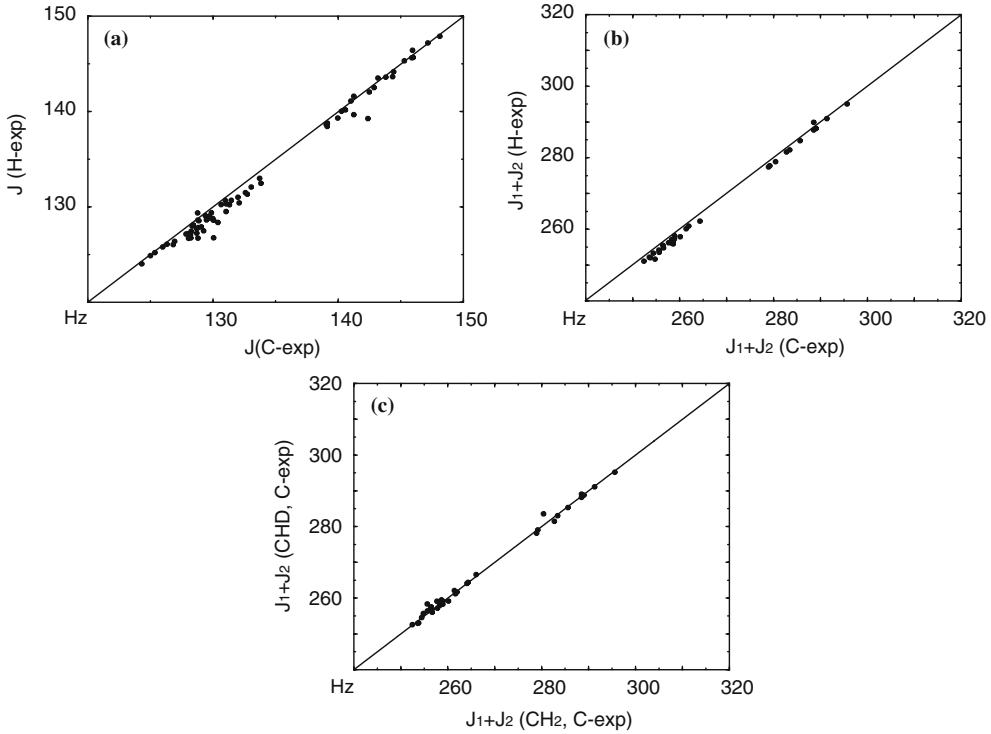

Figure 7. Effect of removing one proton by deuteration in J couplings obtained from the H-exp and C-exp in methylene groups. (a) Comparison of J from the H-exp and C-exp of CHD groups. (b) Comparison of the sum of J for CH^1D and CDH^2 groups from the H-exp and $J_1 + J_2$ of CH_2 groups from the C-exp. (c) J values of CH_2 groups versus the sum of J couplings of CH^1D and CDH^2 groups obtained with the C-exp. Note that for methylene moieties only the sum of both couplings is obtained using the C-exp.

simulation of the intensity by applying Equation 7. In column 5 we report the J values obtained by fitting the simulated intensity to Equation 2. The differences in J from columns 3 and 5 represent approximated values of the error in the H-exp by considering cross-correlated relaxation, $^1H^i$–$^{13}C^i_{DD}/^1H^i$–$^1H^j_{DD}$, as the dominant source of error in the measurement. The estimated errors are similar in sign and magnitude to the experimentally observed ones even when average values of the cross-correlated relaxation rate and J(^{1}H–^{1}H) are used. For a constant time of 18 and 28 ms, the average errors experimentally determined are 4.5 Hz (Figure 4b) and 8.9 Hz (Figure 5b), respectively, by comparison to the C-exp. The data in Table 1 explain the increase in J values of CH_2 groups obtained from the H-exp at longer constant time periods (Figure 5b). The last two rows of Table 1 show that the error is independent on the value of J used to simulate the intensity, provided the rest of the parameters are constant. Therefore, for an initial J of 140 or 170 Hz, if the cross-correlated relaxation rate, the constant time 2δ, and the ^{1}H–^{1}H geminal J are identical, the error transferred to the measurement through cross-correlation will be the same.

Data in Table 1 also indicate that the error in the one-bond J(C–H) depends on the value of the geminal ^{1}H–^{1}H coupling. This already implies that the error transferred to the J(C–H) + RDC(C–H) measurement under anisotropic conditions will depend on the value of J(^{1}H–^{1}H) + RDC(^{1}H–^{1}H) according to Equation 7. Therefore, the error in isotropic media, where RDC(^{1}H–^{1}H) equals 0, will be different from that in anisotropic conditions. This explains the different RDC values of methylene groups when comparing the H-exp vs. the C-exp (Figure 8b), assuming that the error in the C-exp is negligible (*vide infra*). In fact the largest interaction present in methylene moieties in the C-exp is originated by dipole–dipole cross-correlated relaxation described in 2.C (Figure 2d). We calculate with Equation 15, $\Gamma_{CiHi1/CiHi2} \approx -9.6$ Hz for ubiquitin at 308 K in the absence of internal

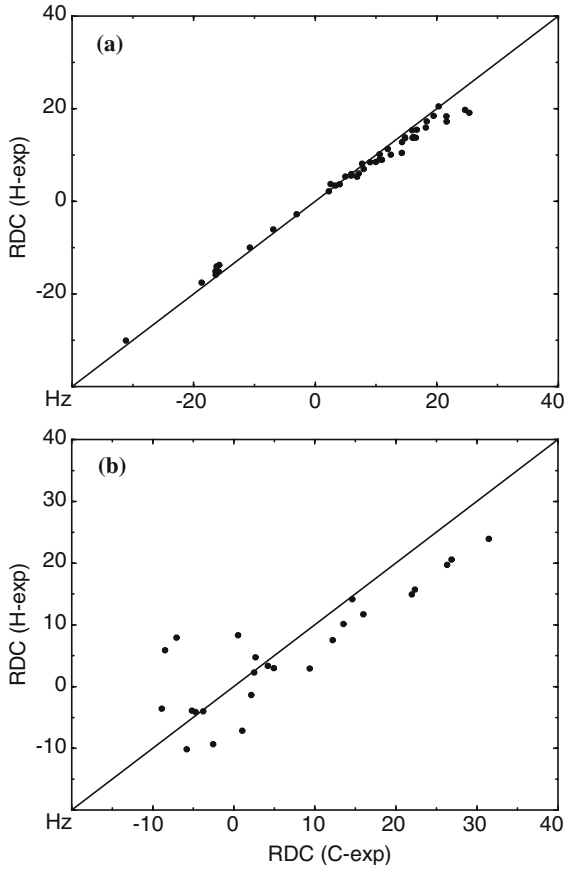

Figure 8. Comparison of residual dipolar couplings of (a) methine and (b) methylene groups obtained from the H-exp and C-exp. For methylene groups the two RDC obtained from the H-exp are added to allow comparison with the C-exp.

motions. By applying Equation 14 the calculated error caused by this pathway of magnetization transfer is zero. This result is not surprising since the cross-correlated relaxation terms in Equation 14 do not depend on λ. Therefore only the amplitude of the modulation, but not its periodicity is modified. Figure 7c shows that J couplings of CH_2 and CHD groups obtained from the C-exp are very similar, in agreement with the previous explanation.

The influence of J(^{1}H–^{1}H) in the magnitude of the error is as well manifested in the results obtained for the CH_3 groups. The average difference between J values from the H-exp and C-exp for methyl moieties is 1.1 Hz (data not shown), similar in magnitude and sign to that observed for CH sites. J(^{1}H–^{1}H) between protons belonging to the same methyl group is zero. Therefore, the

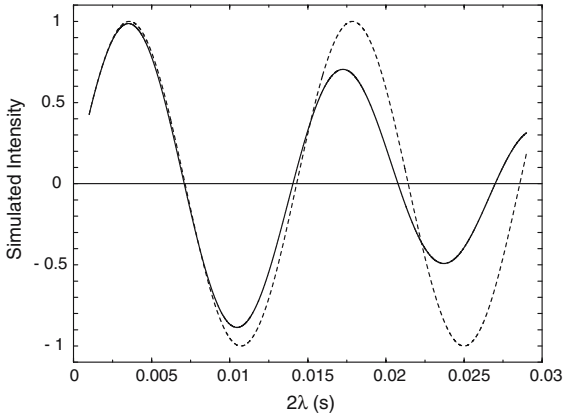

Figure 9. Simulation of intensity modulation with time using a sine dependence ($sin2\pi J\lambda$) and Equation 7. The continuous line represents the modulation that considers cross-correlated relaxation (Equation 7). The dashed line does not include the contribution from cross-correlated relaxation (sin $2\pi J\lambda$). Parameters used in the simulation are J(C–H) = 140 Hz, ^{2}J(H–H) = −15 Hz, $2\delta = 17.8$ ms, $S^2 = 0.77$ (Jin et al., 2003), $\tau_c = 3.33$ ns (Chang and Tjandra, 2005), $\Theta = 35.5°$, $d_{Ci\text{-}Hi} = 1.09$ Å, $d_{Hi\text{-}Hj} = 1.76$ Å (Tjandra et al., 1997), $\Gamma_{HiCi/HiHj} = 9.7$ Hz.

second term of Equation 7 will be zero. The amplitude but not the periodicity of the modulated intensity can change by DD–DD process illustrated in Figure 2a for methyl groups. Magnetization cannot be transferred through cross-correlated relaxation in the same fashion as in methylene moieties.

Following a similar procedure as that used to obtain the data reported in Table 1, we have estimated the error incorporated into the measurement of one-bond J(C–H) for several CH_2 groups of the protein ubiquitin (Table 2), including alpha and beta moieties with different previously reported S^2 values. For residues G_{35} and G_{47} we have assumed a S^2 value of 0.85 since the experimentally calculated values are not reported. The data in Table 2 show that nearly all scalar couplings of CH_2 groups corrected for the interference of cross-correlated relaxation are closer to those experimentally determined for CHD groups.

Analysis of the interference between cross-correlated relaxation and J values for methine moieties

For CH groups it is not possible to identify *a priori* one dominant pathway of cross-correlated relaxation. Therefore, in order to simplify the analysis we have calculated the error transferred to the

Table 1. Error (J_{sim}–J_{CiHi}) transferred to an ideal J_{CiHi} by fitting simulated intensity[d] of CH_2 groups affected by cross-correlated relaxation (Equation 7, Figure 2a) to Equation 2.

$\Gamma_{HiCi/HiHj}$ (Hz)	2δ (ms)	J_{CiHi} (Hz)	J_{HiHj} (Hz)	J_{sim} (Hz)
9.7[a]	17.8	140.0	−10.0	142.0
			−15.0	143.4
9.7[a]	28.0	140.0	−10.0	143.5
			−15.0	149.8
12.0[b]	17.8	140.0	−17.6[c]	145.6
		170.0	−17.6[c]	175.6

[a, b]Parameters used to calculate $\Gamma_{HiCi/HiHj}$ with Equation 15 are: $\tau_c = 3.33$ ns (Chang and Tjandra, 2005), $\Theta = 35.5°$, $d_{Ci\text{-}Hi} = 1.09$ Å, $d_{Hi\text{-}Hj} = 1.76$ Å (high resolution NMR structure of ubiquitin reported by Tjandra et al., 1997), [a]$S^2 = 0.77$ (average S^2 value for CH_2 groups reported by Jin et al., 2003), [b]$S^2 = 0.88$ (S^2 value reported for ubiquitin G_{10} by Jin et al., 2003).
[c]J_{HiHj} data for ubiquitin G_{10} reported by Carlomagno et al. (2000).
[d]Simulated intensities in Tables 1, 2 and 3 were obtained with Mathematica (Wolfram, 1991).

measurement of $J(C^{\alpha}–H^{\alpha})$ in the H-exp for two particular residues of ubiquitin which contain a single $^1H^{\beta}$. The data are reported in Table 3. The cross-correlated relaxation rates were calculated using Equation 15. The error shown in column 4 of Table 3 was obtained by fitting to Equation 2 the simulated intensity obtained with Equation 8. Other parameters such as $^3J(H^{\alpha}–H^{N})$ values were measured and $^3J(H^{\alpha}–H^{\beta})$ data have been reported previously (Delaglio et al., 2001). We show that the error (column 4 of Table 3) can be either positive or negative depending on the sign of the cross-correlated relaxation rate, and is smaller than the average 0.8 Hz experimentally observed. J values obtained from the H-exp and the C-exp are reported in columns 5 and 6.

We have estimated that other processes of cross-correlated relaxation described in 1.D can add an error of ±0.1 Hz to the one-bond J(C–H), by calculating $\Gamma_{H^{\alpha}C^{\alpha}/H^{\alpha}C^{\beta}} = 0.96$ Hz and assuming a $^2J(H^{\alpha}–C^{\beta}) = \pm 5$ Hz.

Cross-correlation also affects scalar couplings measured from ^{13}C magnetization, as can be inferred from the description of magnetization evolution for the C-exp (*vide supra*). For cross-correlated relaxation pathways indicated in 2.C and illustrated in Figure 2c, we have calculated an upper limit of $\Gamma_{H^{\alpha}C^{\alpha}/H^{\beta}C^{\alpha}} = -1.6$ Hz and $\Gamma_{H^{\alpha}C^{\alpha}/H^{N}C^{\alpha}} = 0.8$ Hz. Assuming two-bond scalar couplings of $^2J(C^{\alpha}–H^{\beta}) = \pm 5$ Hz or $^2J(C^{\alpha}–H^{N}) = \pm 5$ Hz, and using Equation 12 the estimated error transferred to J is ±0.2 Hz.

In addition to the effects of cross-correlated relaxation by magnetization transfer, scalar couplings are affected by the presence of dynamic frequency shifts (Werbelow, 1996). Equations 5 and 10 indicate how this parameter modifies the value of J measured from the H-exp and the C-exp, respectively. An approximated value of the dynamic frequency shift can be calculated using the following equation (Werbelow, 1996):

$$\mathrm{DFS}(I_{CSA}/IS_{DD}) \approx -(1/10\pi)(\mu_0/4\pi)(h/2\pi)\sigma_I\gamma_I\gamma_S \times (d_{I-S})^{-3}(3\cos^2\theta - 1)1/(1+1/(\omega_I\tau_c)^2) \quad (16)$$

where, τ_c is the overall correlation time of the protein, μ_0 is the susceptibility of the vacuum, γ_I and γ_S, are the gyromagnetic ratios of nuclei I and S, respectively, $d_{I\text{-}S}$ is the distance between nuclei I and S, θ is the angle between the principal axes of the CSA and DD interactions, σ_I is the parallel minus perpendicular components of the I CSA tensor, and ω_I is the angular Larmor frequency of I. In Equation 16 it is assumed that the motion is completely isotropic and the effect of internal dynamics is not considered.

By subtracting Equation 5 from 10, the difference in J from the C-exp and the H-exp, in the absence of other interactions, is DFS ($^{13}C_{CSA}/^1H–^{13}C_{DD}$). We assume $\theta = 0°$, $d_{H\text{-}C} = 1.09$ Å, $\tau_c = 3.33$ ns (Chang and Tjandra, 2005), and an average $\sigma_{13C} = -25$ ppm. This average value corresponds to residues adopting β-structure, which is the most abundant secondary structure of ubiquitin, and is larger than the average value for amino acids in the α-helical conformation (Tjandra and Bax, 1997b). With Equation 16 we calculate DFS ($^{13}C_{CSA}/^1H–^{13}C_{DD}$) ≈ 0.22 Hz. The J values obtained from the C-exp will be in average ~0.22 Hz larger than from the H-exp because of dynamic frequency shifts. This result does not account for the experimentally observed difference of 0.8 Hz.

Dynamic frequency shifts also interfere with J values of methylene moieties, but this effect can be considered negligible in comparison to the experimental average variation (4.5 Hz).

Another factor to take into account is the change in the relaxation rate of the collected operator due to the transfer of magnetization from

Table 2. Comparison of J values ($J_{corr(i)}$ and $J_{corr(j)}$) for CH_2 groups corrected for the effect of cross-correlated relaxation to experimental values ($J_{exp(i)}$ and $J_{exp(j)}$) of CHD groups from the H-exp.

Resid.	S^2	$\Gamma_{HiCi/HiHj}$ (Hz)[a]	J_{HiHj} (Hz)	$Error_{sim}$ (Hz)	$J_{exp(i)}$ CH_2	$J_{exp(j)}$ CH_2	$J_{corr(i)}$ CH_2	$J_{corr(j)}$ CH_2	$J_{exp(i)}$ CHD	$J_{exp(j)}$ CHD
G_{10}	0.88[b]	12.0	−17.6[c]	5.6	146.9	145.3	141.3	139.7	142.1	140.3
G_{35}	0.85	11.6	−16.5[c]	4.8	148.0	147.3	143.2	142.5	143.7	141.2
G_{47}	0.85	11.6	−17.6[c]	5.5	147.3	146.3	141.8	140.8	141.6	140.6
N_{25}	0.82[b]	11.3	−12.6	3.0	132.8	131.5	129.8	128.5	131.7	128.9
N_{60}	0.50[b]	6.9	−13.9	2.2	134.5	132.4	132.3	130.2	132.3	130.5

Column 3: calculated cross-correlated relaxation rate using Equation 15. [a]$\Gamma_{HiCi/HiHj}$ values were calculated with the structural parameters indicated in the caption of Table 1 (Tjandra et al., 1997).
[b]S^2 values reported by Jin et al. (2003). Column 4: experimentally measured ^1H–^1H geminal J values for the corresponding residues. [c]J_{HiHj} data reported by Carlomagno et al. (2000). Column 5: error derived by subtracting the real J value from the J value obtained by fitting to Equation 2 the simulated intensity calculated using Equation 7. Columns 6 and 7: experimentally measured J values from the H-exp using Equation 2 to fit the intensity modulation. Columns 8 and 9: corrected J value by subtracting the error of column 5 from the values reported in columns 6 and 7. Columns 10 and 11: experimentally measured J values of the corresponding residues in CHD groups, where the effect of cross-correlated relaxation that is being analyzed is absent.

Table 3. Estimated error ($Error_{sim}$) transferred to $J(C^{\alpha}–H^{\alpha})$ in the H-exp by cross-correlated relaxation. Comparison of the experimental $J(C^{\alpha}–H^{\alpha})$ values from the H-exp ($J_{(H\text{-}exp)}$) and the C-exp ($J_{(C\text{-}exp)}$).

Residue	$\Gamma_{H^{\alpha}C^{\alpha}/H^{N}H^{\alpha}}$ (Hz)[a]	$\Gamma_{H^{\alpha}C^{\alpha}/H^{\beta}H^{\beta}}$ (Hz)[a]	$Error_{sim}$ (Hz)[b]	$J_{(H\text{-}exp)}$ (Hz)	$J_{(C\text{-}exp)}$ (Hz)
I_3	−0.29	−1.63	+0.1	139.2	139.9
T_{14}	−0.28	2.99	−0.4	142.6	143.6

[a]$\Gamma_{HiCi/HiHj}$ values were calculated using Equation 15 with the structural parameters indicated in the caption of Table 1 (Tjandra et al., 1997) and assuming $S^2 = 0.85$.
[b]Three-bond ^1H–^1H J data are needed to estimate the error. $^3J(H^{\alpha}–H^{N})$ values were measured and $^3J(H^{\alpha}–H^{\beta})$ values are reported by Delaglio et al. (2001).

an operator that might have a different relaxation rate. In fact, the operators that transfer magnetization, for example in Equation 8, are of the type $2H_x^iH_z^j$, which relax ~6 Hz faster than the collected operator $2H_x^iC_z^i$, due to ^1H–^1H dipolar interactions (Vuister and Bax, 1993). By taking into account this effect in Equation 8, J values decrease by less than 0.1 Hz. This result indicates that a change in the relaxation rate of the collected operator does not account for the difference observed in J(C–H) of methine groups of the H-exp and C-exp.

A combination of all possible interactions together with a leakage of magnetization more probable to occur in the H-exp than the C-exp, due to the intrinsic relaxation properties of the ^1H vs. ^{13}C nucleus, might account for the 0.8 Hz difference between both types of experiments. This systematic error seems to cancel when obtaining RDC, and the small deviations observed in the H-exp vs. the C-exp (Figure 8a) are probably due to different errors in the isotropic and anisotropic media originated from cross-correlated relaxation.

Conclusions

By comparing scalar and dipolar couplings of methylene groups obtained from ^1H and ^{13}C magnetization with the Quantitative J method, we have been able to analyze the interference between cross-correlated relaxation and J coupling measurements. We show that the magnitude of the experimentally observed error can be estimated by the theoretical equations describing this phenomenon. In the Quantitative J experiment that monitors a single operator, the interference of cross-correlated relaxation is explained as a transfer of magnetization between operators that modifies the periodicity of the signal intensity modulation and as dynamic frequency shifts.

The magnitude of the error added to the J by magnetization transfer depends on the cross-

correlated relaxation rate, on the J values that relate the interacting spins, as well as on the time during which scalar coupling and cross-correlated relaxation are active.

J + RDC measurements in anisotropic media are also affected by an error, which is different from that present under isotropic conditions. Therefore, the error does not cancel when obtaining RDC as subtraction of measurements performed under isotropic and anisotropic conditions. In contrast, the effect of dynamic frequency shifts cancels in RDC values.

The interference between cross-correlation and scalar couplings is enhanced in the proton vs. the carbon, since this nucleus is prone to have larger cross-correlated relaxation rates, and because its proximity to other nuclei acting as relaxation pathways. The cross-correlated relaxation rate depends on the correlation time. Therefore, for large biomolecules, even when ^{13}C magnetization is monitored, cross-correlation might interfere with studies of detailed structural geometry that require precise J and RDC measurements. However, for the general application of these parameters to structure determination, the interference between cross-correlated relaxation and J measurement will probably not affect the resulting structure. Nevertheless, the use of selective pulses can suppress some of these effects by refocusing the evolution of magnetization with cross-correlated relaxation.

Electronic supplementary material is available in electronic formatt at http://dx.doi. org/10.1007/s10858-006-0028-4

Acknowledgements

We are grateful to Drs. Dennis Torchia, Ad Bax and Rieko Ishima for useful suggestions. We specially thank Professor Larry Werbelow for sharing with us important information related to dynamic frequency shifts and for pointing out the simplification made by separating internal dynamics from the relative orientation of the corresponding interactions in the equation for the cross-correlated relaxation rate. We are indebted to Professor Christian Griesinger for the clarification of some aspects in relation to cross-correlated relaxation.

References

Bachmann, P., Aue, W.P., Müller, L. and Ernst, R.R. (1977) *J. Magn. Reson.*, **28**, 29–39.
Bax, A., Vuister, G.W., Grzesiek, S., Delaglio, F., Wang, A.C., Tschudin, R. and Zhu, G. (1994) *Meth. Enzymol.*, **239**, 79–105.
Bax, A., Kontaxis, G. and Tjandra, N. (2001) *Meth. Enzymol.*, **339**, 127–174.
Bax, A. and Grishaev, A. (2005) *Curr. Opin. Struct. Biol.*, **15**, 563–570.
Boisbouvier, J. and Bax, A. (2002) *J. Am. Chem. Soc.*, **124**, 11038–11045.
Boyd, J., Soffe, N., John, B., Plant, D. and Hurd, R. (1992) *J. Magn. Reson.*, **98**, 660–664.
Bull, T.E. (1991) *J. Magn. Reson.*, **93**, 596–602.
Bystrov, V.F. (1976) *Prog. NMR Spectrosc.*, **10**, 41–81.
Carlomagno, T., Felli, I.C., Czech, M., Fischer, R., Sprinzl, M. and Griesinger, C. (1999) *J. Am. Chem. Soc.*, **121**, 1945–1948.
Carlomagno, T., Peti, W. and Griesinger, C. (2000) *J. Biomol. NMR*, **17**, 99–109.
Carlomagno, T., Bermel, W. and Griesinger, C. (2003) *J. Biomol. NMR*, **27**, 151–157.
Chang, S.-L. and Tjandra, N. (2005) *J. Magn. Reson.*, **174**, 43–53.
Chiarparin, E., Pelupessy, P., Ghose, R. and Bodenhausen, G. (1999) *J. Am. Chem. Soc.*, **121**, 6876–6883.
Davis, A.L., Keeler, J., Laue, E.D. and Moskau, D. (1992) *J. Magn. Reson.*, **98**, 207–216.
De Alba, E. and Tjandra, N. (2002) *Prog. NMR Spectrosc.*, **40**, 175–197.
Delaglio, F., Grzesiek, S., Vuister, G.W., Zhu, G., Pfeifer, J. and Bax, A. (1995) *J. Biomol. NMR*, **6**, 277–293.
Delaglio, F., Wu, Z. and Bax, A. (2001) *J. Magn. Reson.*, **149**, 276–281.
Ernst, M. and Ernst, R.R. (1994) *J. Magn. Reson. (Series A)*, **110**, 202–213.
Garrett, D.S., Powers, R., Gronenborn, A.M. and Clore, G.M. (1991) *J. Magn. Reson.*, **95**, 214–220.
Ghose, R. and Prestegard, J.H. (1998) *J. Magn. Reson.*, **134**, 308–314.
Griesinger, C., Sörensen, O.W. and Ernst, R.R. (1986) *J. Chem. Phys.*, **85**, 6837–6843.
Grzesiek, S., Kuboniwa, H., Hinck, A.P. and Bax, A. (1995) *J. Am. Chem. Soc.*, **117**, 5312–5315.
Harbison, G.S. (1993) *J. Am. Chem. Soc.*, **115**, 3026–3027.
Jin, C., Prompers, J.J. and Brüschweiler, R. (2003) *J. Biomol. NMR*, **26**, 241–247.
Kay, L.E., Keifer, P. and Saarinen, T. (1992) *J. Am. Chem. Soc.*, **114**, 10663–10665.
Kroenke, C.D., Loria, J.P., Lee, L.K., Rance, M. and Palmer, A.G. III (1998) *J. Am. Chem. Soc.*, **120**, 7905–7915.
Lazar, G.A., Desjarlais, J.R. and Handel, T.M. (1997) *Prot. Sci.*, **6**, 1167–1178.
Lipari, G. and Szabo, A. (1982) *J. Am. Chem. Soc.*, **104**, 4546–4559.
Miclet, E., Williams, D.C., Clore, G.M., Bryce, D.L., Boisbouvier, J. and Bax, A. (2004) *J. Am. Chem. Soc.*, **126**, 10560–10570.
Ottiger, M., Delaglio, F., Marquardt, J.L., Tjandra, N. and Bax, A. (1998) *J. Magn. Reson.*, **134**, 365–369.

Prestegard, J.H., Al-Hashimi, H.M. and Tolman, J.R. (2000) *Q. Rev. Biophys.*, **33**, 371–424.
Prestegard, J.H., Bougault, C.M. and Kishore, A.I. (2004) *Chem. Rev.*, **104**, 3519–3540.
Rexroth, A., Schmidt, P., Szalma, S., Geppert, T., Schwalbe, H. and Griesinger, C. (1995) *J. Am. Chem. Soc.*, **117**, 10389–10390.
Rief, B., Hennig, M. and Griesinger, C. (1997) *Science*, **276**, 1230–1233.
Riek, R., Wider, G., Pervushin, K. and Wüthrich, K. (1999) *Proc. Natl. Acad. Sci. USA*, **96**, 4918–4923.
Santoro, J. and King, G.C. (1992) *J. Magn. Reson.*, **97**, 202–207.
Schwalbe, H., Carlomagno, T., Hennig, M., Junker, J., Reif, B., Richter, C. and Griesinger, C. (2001) *Meth. Enzymol.*, **338**, 35–81.
Shaka, A.J., Barker, P.B. and Freeman, R. (1985) *J. Magn. Reson.*, **64**, 547–552.
Silver, M.S., Joseph, R.I. and Hoult, D.I. (1984) *J. Magn. Reson.*, **59**, 347–351.
Sörensen, O.W., Eich, G.W., Levitt, M.H., Bodenhausen, G. and Ernst, R.R. (1983) *Prog. NMR Spectrosc.*, **16**, 163–192.
Tessari, M., Vis, H., Boelens, R., Kaptein, R. and Vuister, G.W. (1997) *J. Am. Chem. Soc.*, **119**, 8985–8990.
Tjandra, N., Szabo, A. and Bax, A. (1996) *J. Am. Chem. Soc.*, **118**, 6986–6991.
Tjandra, N. and Bax, A. (1997a) *J. Magn. Reson.*, **124**, 512–515.
Tjandra, N. and Bax, A. (1997b) *J. Am. Chem. Soc.*, **119**, 9576–9577.
Tjandra, N., Omichinski, J.G., Gronenborn, A.M., Clore, G.M. and Bax, A. (1997) *Nat. Struct. Biol.*, **4**, 732–738.
Tolman, J.R., Chung, J. and Prestegard, J.H. (1992) *J. Magn. Reson.*, **98**, 462–467.
Tolman, J.R. and Prestegard, J.H. (1996) *J. Magn. Reson.*, **112**, 245–252.
Vuister, G.W., Delaglio, F. and Bax, A. (1993) *J. Magn. Reson.*, **3**, 67–80.
Vuister, G.W. and Bax, A. (1993) *J. Am. Chem. Soc.*, **115**, 7772–7777.
Werbelow, L.G. (1987) *J. Magn. Reson.*, **71**, 151–153.
Werbelow, L. G. (1996) In *Encyclopedia of Nuclear Magnetic Resonance*, Grant, D.M., Harris, R.K. (Editors-in-Chief), Wiley, London, Vol. 6, pp. 4072–4078.
Wimperis, S. and Bodenhausen, G. (1989) *Mol. Phys.*, **66**, 897–919.
Wolfram, S. (1991) *Mathematica*, Addison-Wesley Publishing Co., Redwood City, CA.